INTERPRETATION OF THE COMMONLY OBSERVED I-V CHARACTERISTICS OF C-SI CELLS HAVING IDEALITY FACTOR LARGER THAN TWO

O. Breitenstein,[1] P. Altermatt,[2,3] K. Ramspeck,[3] M.A. Green,[4] Jianhua Zhao,[4] A. Schenk[5,6]

[1] Max Planck Institute of Microstructure Physics, Weinberg 2, D-06120 Halle, Germany
[2] University of Hannover, Inst. Solid-State Physics, Dep. Solar Energy, Appelstr. 2, D-30167 Hannover, Germany
[3] Institute for Solar Energy Research Hameln (ISFH), Am Ohrberg 1, D-31860 Emmerthal, Germany
[4] Centre for Photovoltaic Engineering, University of New South Wales, Sydney 2052, Australia
[5] Integrated Systems Laboratory, ETH Zurich, Gloriastr. 35, 8092 Zurich, Switzerland
[6] Synopsys Switzerland LLC, Affolternstr. 52, 8050 Zurich, Switzerland

ABSTRACT

The dark I-V characteristics of crystalline silicon solar cells usually deviate from that expected by classical diode theory by an unusually high ideality factor and magnitude at biases smaller than about 0.5 V. It had been shown that the recombination current is flowing preferentially in certain local extended defect positions like the edge or local shunts. There, the local density of recombination centers in the pn-junction is higher than in the bulk by orders of magnitude. In this work, we go beyond the SRH theory to explain the recombination effects occurring in such heavily damaged pn-junction regions. Firstly, we apply the coupled defect recombination via two shallow (or one shallow and one deep) level, which explains the observed high ideality factors due to trap-assisted tunneling. Secondly, we apply the coupling of two defects to recombination via deep donor-acceptor pairs, which cause the high ideality factors due to saturation of the recombination rate between the two defects. Thirdly, the local extension of the recombination region across the edge of the cell (due to electrostatic charging) is an other explanation of very high recombination currents.

INTRODUCTION

It is well known since many years that the dark I-V characteristics of most silicon solar cells, especially of industrial ones, deviate from that expected by classical diode theory. One characteristic deviation occurs at biases smaller than about 0.5 V, where the recombination current is orders of magnitude higher than expected from the carrier lifetime obtained at higher biases, and the ideality factor greatly succeeds 2, which cannot be explained by the SRH theory [1-4]. Moreover, even in the absence of obvious ohmic shunts, the characteristics always contain a certain ohmic contribution. Therefore, their reverse characteristic is not of a saturation-type, as expected for classical diode theory, but rather linear or even superlinear. A large ideality factor of a recombination current physically means that the effective recombination lifetime in the depletion layer increases with increasing recombination rate. Hence a recombination mechanism, which gradually saturates with increasing bias, is necessary to explain a large ideality factor. Previous attempts to interpret large ideality factors, e.g. based on trap-assisted tunneling or field-enhanced recombination via single levels, were based on the assumption of a recombination current flowing homogeneously across the cell [3]. However, these interpretations were not very convincing, since they were not compatible with existing lifetimes and point defect parameters. Also the coupled defect-level model [5] was originally introduced by assuming a homogeneous spatial distribution of defects.

It had been suspected already very early [6] that such non-ideal recombination currents are flowing not homogeneously but rather in local sites of certain extended defects, for which originally metallic precipitates were suspected. Lock-in thermography (LIT) [7-11] is the technique of choice to image the inhomogeneity of the dark current in solar cells. In this technique a pulsed bias is applied to the cell in the dark, the cell is imaged by a highly sensitive infrared camera connected to a computer system, and the incoming images are processed and averaged on-line according to the lock-in principle [11]. Within the spatial resolution limit of this technique, which is given by the frequency-dependent thermal heat diffusion length being in the order of 1 mm, the local temperature modulation amplitude is proportional to the locally dissipated power density. Hence, if LIT is performed at different biases, it also allows to measure local I-V characteristics locally in a non-destructive way [8] and even allows to create an image of the local ideality factor [9]. Already an early variant of LIT working with point-by-point contact temperature measurements (DPCT [7,8]) had proven that most of the recombination current (and of the ohmic current contribution) is flowing at the edge of the cell and in certain shunt positions. Thermal ideality factor mapping has proven that in multicrystalline solar cells the low lifetime regions are characterized by an increased diffusion current density, but still show an ideality factor close to 1 [9]. Only the edge regions and local shunts are characterized by an ideality factor larger than 2. Independently, several groups have realized by I-V measurements on differently sized cells that the recombination current is essentially an edge current [12, 13]. McIntosh et al. [13] have attributed the large ideality factor of the edge current to the series resistance in the emitter, still assuming conventional edge recombination via point defect levels. However, for series resistance effects to become effective, relatively high current-densities are necessary, which usually only arise at a bias above 300 mV. Most non-ideal solar cells, however, have a large ideality factor over a large bias range, starting already below 100 mV. Moreover, if only a recombining interface is assumed that crosses the pn-junction, the thermal velocity of free carriers sets a limit to the saturation current to about 10^{-8} A/cm [14]. However, in many cases, measured edge currents exceed this limit.

A nearly ideal dark IV characteristic (with an ideality factor close to 1) down to 0 V has been found in "passivated emitter, rear locally-diffused" (PERL) and "passivated emitter, rear totally-diffused" (PERT) cells.. The main reason for this ideal behaviour is that the edges of the cells are lying well passivated below a high-quality oxide. However, some PERL cells exhibit a high ideality factor, and we have shown by LIT investigations [10] that this recombination current is due to local shunting.

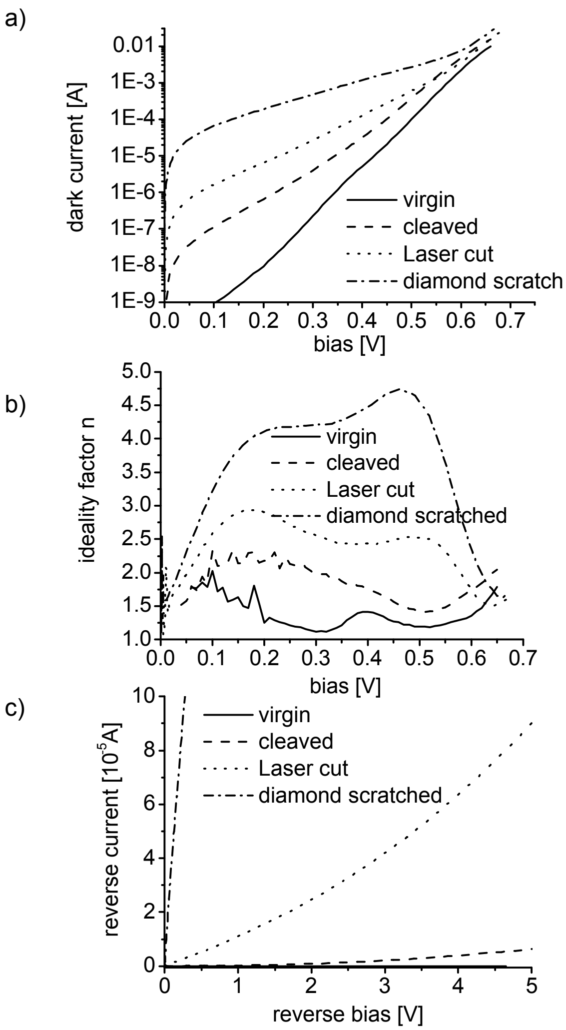

Fig. 1: (a) Forward I-V characteristics, (b) bias-dependent ideality factors, and (c) reverse I-V characteristics (in linear drawing) of a typical virgin PERT cell and of 3 cells with different mechanical processing.

In the following section we will demonstrate the conversion of the ideal I-V characteristics into non-ideal ones by cutting the pn-junction of ideal PERT cells by different means. Based on these measurements, we will present three mechanisms that lead to the observed high currents and ideality factors larger than 2 for biases <0.5V.

ARTIFICIAL GENERATION OF NON-IDEAL I-V CHARACTERISTICS

We have noticed by DPCT and LIT imaging that scratches at the surface of a solar cell lead to non-linear shunts, which are most probably recombination-induced. Here we apply 3 different techniques to cut the surface of individual PERT cells that originally showed an ideal I-V characteristic: 1. by cleaving along (100), 2. by laser cutting, and 3. by diamond scratching. This allows us to study the influence of this damage on the dark I-V characteristic. Fig. 1 shows the forward characteristics (a), the bias-dependent ideality factor of the forward characteristic (b), and the reverse characteristics (c) of a typical virgin cell and of the 3 processed cells. They are all converted into typical non-ideal ones, but to a different degree. The weakest recombination current was generated by the cleavage process, the laser cut produced a higher current contribution, and the diamond scratch produced the largest current-increase. There is a clear correlation between the magnitude of the recombination current and the ideality factor: The higher the current, the larger the ideality factor. Obviously, these different techniques differ in the density of recombination states, which they produce at the freshly created surfaces crossing the pn-junction. Also the ohmic reverse conductivity clearly correlates with this density of states. In all cases, the artificial defects could be easily imaged by LIT.

INTERPRETATION OF NON-IDEAL I-V CHARACTERISTICS

As mentioned above, the Shockley-Rerad-Hall (SRH) theory cannot explain ideality factors *m*>2 over the entire bias range between 0 and about 0.5 V [1,2]. We need to keep in mind that the SRH theory assumes that the defects act as *isolated* recombination centers. This condition breaks down at very high defect densities, because the wavefunctions of neighboring defects overlap spatially. This leads to electronical coupling of at least two neighboring centers (if not of several centers), which opens up at least two main path ways for recombination:
(i) The wave functions of *shallow defects* come close to the band edge in non-neutral regions, as is shown in Fig. 2a. If such defects are isolated, the tunneled electron simply becomes thermally emitted into the band edge again, making recombination very improbable. However, if the tunneled electron gets immediately transferred to a deeper lying state, its probability for recombination is very high. This recombination path has been called coupled defect-level recombination [5].
(ii) *Deep centers* interact very little with each other at usual defect densities, due to their constricted wavefunctions, but at very high defect densities they can do. Hence, an

electron captured at a deep donor-like defect can be transferred immediately to an acceptor-like defect, where the probability for recombination can be very high, see Fig. 2b. This recombination path has been historically called donor-acceptor-pair (DAP) recombination.

We like to emphasize that the two recombination paths are two different limiting cases of one and the same model: The first one has its bottleneck in the phonon-coupling of the tunneled electron to the excited state, while the second one has its bottleneck in the transfer rate between the two deep defects. Both bottlenecks cause the desired saturation of the recombination current with higher bias.

Because m>2 is very frequently observed at low bias, our models must produce such a ideality factor in a broad range of defect parameters; otherwise, m>2 would be observed only in special circumstances. In our model, both limiting cases require commonly found defect parameters. However, we do not know yet whether shallow or deep defects predominate in which circumstances.

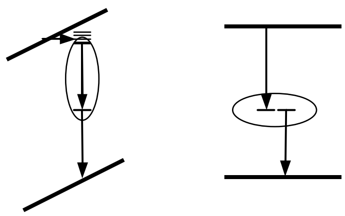

Fig. 2: Trap-assisted tunneling into an excited defect state, followed by a transfer of the electron to a second, deeper defect (left). Transfer of the electron between acceptor- and donor-like deep defects, which also may have different energies (right). The coupling between the two defects is symbolized by the ellipsis.

Coupled defect-level model

This model had been published already in 1995 [5] and was originally developed to interpret measured I-V characteristics of LPE-grown silicon solar cells, based on the assumption of a homogeneous recombination current flow. Since in this model at least one of the recombination partners must be a shallow level having a larger extension of the wave function, and the doping concentration was not high enough to account for the measured magnitude of the recombination current, it was suspected there that shallow impurities are accumulating at the epitaxial interface, which was lying in the depletion region in these cells. However, such an assumption is not necessary anymore if the recombination current is flowing locally in the sites of extended defects showing a high local density of states. Note that at the surface of a diamond scratch and even at a cleaved face the silicon material may be locally amorphized. It is well known that amorphous silicon contains density-of-state tails at both band edges, which predominantly consist of shallow levels. Also if some native oxide covers the surface, the interface to this oxide contains a high local density of such states. Hence, even for solar cells with a high lifetime and no accumulation of any point defect levels in the depletion region, the coupled defect-level (CDL) model can be applied in the position of highly recombinative defects crossing the pn-junction.

In this work, the CDL model [5] was used to simulate a PERL cell with the simulator Dessis in 2D, assuming a shunt region with a cross section of 10 μm x 10 μm crossing the pn-junction at a distance of 3.5 μm from the emitter contact. Ideality factors larger than 2 can be obtained with the CDL model, if the band-trap transitions are assumed to be tunnel-assisted (for details of the theory see [5]). The resulting field effect vanishes with rising forward bias which yields the necessary saturation condition. A precondition for the field effect to be efficient is a very weak coupling of the trapped electron/hole to the lattice. This coupling is usually quantified by the so-called lattice relaxation energy $\varepsilon_R = S\hbar\omega_0$, where the Huang-Rhys factor S is a measure of the coupling strength and $\hbar\omega_0$ is the effective phonon energy of the multi-phonon process. Only in the weak coupling limit, tunnel transitions from band states to localized states are significant. Possible defect candidates include singly- or doubly charged “shallow” donors and acceptors. Then, as a second precondition, the inter-level transition rate must be not rate limiting, otherwise the field effect would obviously disappear. These two considerations suggest to restrict the number of model parameters in the following way: The hole lifetime for the upper level τ_{p1} and the electron lifetime for the lower level τ_{n2} are set to infinity (no traffic between conduction band and lower level as well as between valence band and upper level). The inter-level rate τ_{12} is set to 10^{40} in order to mimic very fast, not rate-limiting transitions. Both trap levels are assumed to have the same energetic distance from their respective band edges, i.e. $E_{t1} = E_{t2} = E_t$. The lifetimes τ_{n1} and τ_{p2} are given the same value for simplicity ($\tau_{n1} = \tau_{p2} = \tau$).

In order to reproduce the experimentally observed increasing recombination current $I(V)$ and the increasing “ideality peak” $n(V)$ with stronger local distortion of the lattice, we varied the trap level E_t and the lifetime τ for a fixed small lattice relaxation energy ε_R. An effective phonon energy of 10 meV was chosen which always guarantees that $\hbar\omega_0 << E_t$ (a precondition in multi-phonon theory). Since $\tau \sim 1/N_t$, a reduction of the lifetime corresponds to a growing defect density. This leads, at the same time, to an increase of the recombination current at small forward bias *and* to a broader $n(V)$-peak. However, the magnitude of the maximum of the ideality factor n_{max} cannot be increased significantly by reducing the lifetime. This can only be achieved by increasing the energetic depth E_t of the trap state. Fig. 3 shows the growing nonideal recombination current and the increase of n_{max} from 1.0 to 6.5, if the lifetime is reduced from 10^{-4} sec to $2*10^{-8}$ sec and E_t is increased from 50 meV to 190 meV. In this simulation, the lattice relaxation energy was fixed at 5 meV (i.e. S=0.5). Whereas the physical reason for a decreasing lifetime is obvious, the necessary increase of E_t to obtain a larger n_{max} is less transparent. A possible explanation is given by a change of the effective charge number of the hydrogenic defects from 1 to 2 because the charged defects have overlapping wavefunctions. The increase of E_t is also compatible with the formation of strong tails of the density of states containing deeper lying levels as the lattice distortion becomes stronger.

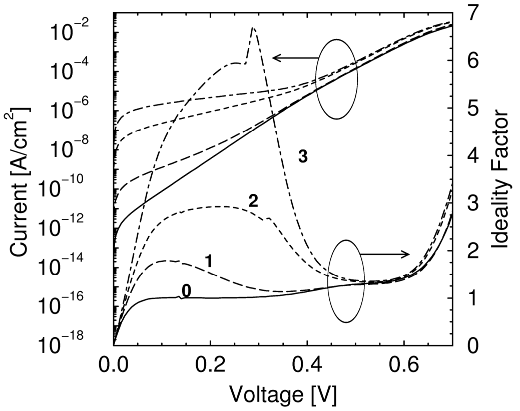

Fig. 3: Simulated forward I-V characteristics and ideality factors of the PERL cell described in the text. 0: E_t = 50 meV, τ = 1e-4 s, 1: E_t = 90 meV, τ = 8e-7 s, 2: E_t = 145 meV, τ = 6e-8 s, 3: E_t = 190 meV, τ = 4e-8 s.

Deep donor-acceptor-pair recombination

In Ref. [5] recombination via two deep levels was not found to give the explanation for ideality factors larger than 2, since the wave function of deep levels is highly localized. Hence, the overlap between the wave functions of two levels, which is necessary for enabling inter-level recombination, is remarkable only for very high local level concentrations, which was considered to be improbable. However, as for the coupled defect level model, this situation changes as soon as extended defects are considered to be responsible for the recombination current. A defect density of 10^{14}cm^{-2}, which is not unrealistic for a non-passivated surface, corresponds to a mean defect distance of 1 nm, which is already in the order of the spatial extension of deep levels. In the coupled defect-level model, the saturation effect comes from a reduction of the tunnel probability with decreasing electric field, but the inter-level recombination was assumed to be not rate-limiting. Here we propose the other case that capture into the levels occurs conventionally, but the inter-level recombination process shows a limited (distance-dependent) probability. The physical mechanism of the saturable recombination current caused by DAP recombination is the following: Donors and acceptors are differing in the charge state of their unoccupied state, leading to very different capture coefficients to electrons and holes. The recombination via isolated deep donors and acceptors in the depletion region is limited by their smaller capture coefficient to holes and electrons, respectively. If recombination between donors and acceptors is allowed, and the DAP recombination coefficient is large enough, hence if the local density of states is high enough, this bottleneck may be bypassed by DAP recombination. This recombination path, however, is saturable, since the number of recombination partners is limited, leading to an ideality factor > 2 for certain biases.

We have solved the rate equations implying two interacting levels similar as in [5] under the following simplifying conditions: There is only one donor and one acceptor level species, which have the same concen-

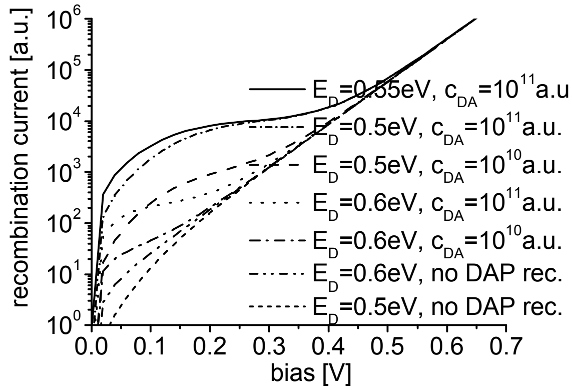

Fig. 4: Modeled forward I-V characteristics (recombination rate) for symmetric DAP recombination for different values of the donor binding energy E_D and of the DAP recombination coefficient c_{DA}.

tration and complementary electronic parameters. Hence, the electron capture cross section of the donor equals the hole capture cross section of the acceptor and vice versa, and the energy distance of the donor to the conduction band equals the distance of the acceptor to the valence band. However, these energy distances are allowed to be larger than $E_g/2$, hence also donors in the lower and acceptors in the upper gap half were allowed. An asymmetry of the capture cross sections of 1:100 was assumed. Under these conditions the rate equations can easily be solved and the expected recombination rates in the center of the depletion region (where n = p) can be calculated. Fig. 4 shows the results for different energy depths of the donor level E_D and for different values of the donor-acceptor-pair recombination probability c_{DA}. Though these results are only in arbitrary units, they already show the expected qualitative behaviour. Without DAP recombination, an ideality factor of 2 or below appears for all energies, as expected. In all other cases considered here, the saturable DAP recombination is leading to regions in the I-V characteristic with lower slope, hence with higher ideality factor. Note that these regions are appearing here already at low biases < 0.1 V, where the resistance-limited edge recombination did not show an effect yet [13]. The influence of DAP recombination is largest for the midgap levels ($E_D = E_A$ = 0.55 eV). For E_D = 0.6 eV (very deep donor) the current is lower because the DAP recombination is thermally activated there. For E_D = 0.5 eV the current is also lower at low bias, since here at low bias the occupancy factor of the levels is lower. This tendency continues for even deeper and shallower levels, hence deep DAP recombination is most effective for midgap levels.

Local extension of the recombination region

The previous models can be implemented e.g. by introducing a 2-dimensional plane containing the corresponding recombination centers perpendicular to the pn-junction as an extended defect. Then, if charging of this plane is not considered, the electric field distribution at this plane is the same as for the undisturbed pn-junction. However, if a high local density of states is present at this extended defect, electric charging is unavoidable, which in turn changes the local field distribution. If the recombination plane is a surface, it will be covered by a native oxide, which contains additional fixed oxide charges. Hence, for realistically modeling a pn-junction crossing a surface, we have to consider both fixed oxide charges at the surface and rechargeable interface states, which also act as recombination centers. It turns out that the formation of a surface inversion layer leads to a local extension of the recombination region from the region within the pn-junction to a considerable part of the surface, as is sketched in Fig. 5.

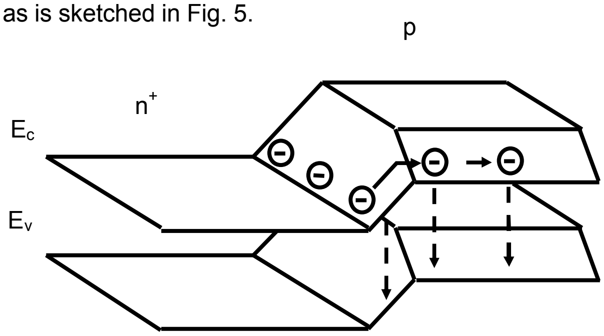

Fig. 5: Sketch of the 3-dimensional band distribution in the position where the pn-junction crosses the surface (in front). The recombination region extends from the pn-junction region (left dashed arrow) across the surface of the p-region (right dashed arrows).

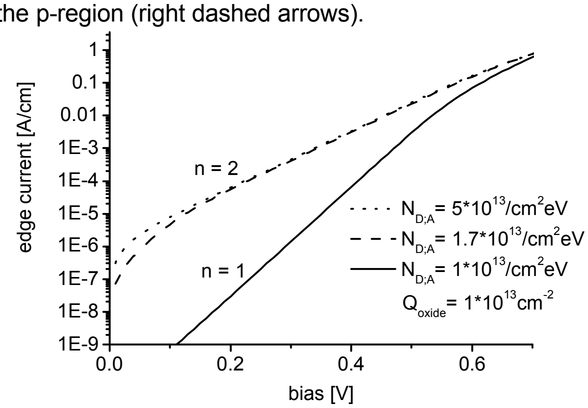

Fig. 6: Edge current densities modeled by Dessis using a continuous distribution of donors and acceptors of the same concentration

The 2-D device simulation program Dessis [15] was used to perform this simulation. A similar simulation was performed already by Kühn et al. [14], assuming a cell thickness of 5 µm and one midgap recombination level at the surface. This simulation lead to a hump in the I-V characteristic. Here we will perform a similar Dessis simulation, assuming a cell thickness of 200 µm, a continuous distribution of donor- and of acceptor-type interface states of the same density, and a higher oxide charge density of 10^{13} cm^{-2}. First results of this simulation are shown in Fig. 6. For the lowest defect density of $10^{13}/cm^2eV$, the surface is completely inverted for all biases, and the edge recombination is negligible. For higher defect densities, the Fermi level is more and more pinned close to midgap, as shown in Fig. 5. With the parameters and the isolated point defect recombination model used here, an ideality factor larger than 2 was not obtained. However, for sufficiently large defect densities, an edge current having J_{02}^{surf} as large as 10^{-6} A/cm was obtained. This proves that the electrostatic charging effect in the edge region is sufficient to explain edge saturation current densities well above 10^{-8} A/cm.

The reverse characteristics

Another non-ideal feature of most silicon solar cells is that, even in the absence of obvious ohmic shunts, their reverse dark I-V characteristic is linear or even superlinear (see Fig. 1 c), instead of saturation-type (sub-linear) as expected in classical diode theory. The blocking characteristic of a pn-junction under reverse bias is generally a consequence of the energy gap of the density of states, which prevents the carriers from flowing through the depletion layer. However, if an extended defect showing a continuous density of interface states is crossing the pn-junction, there is no complete band gap anymore in this position. If the density of interface states in this defect position is high enough that neighbouring wave functions are overlapping, electronic transitions between the states are possible. Since these transitions are expected to occur in the energy position of the Fermi-level in both directions, a certain ohmic conductivity is established in the defect sites between the p- and the n-region. This situation is schematically sketched in Fig. 7. If a higher voltage is applied to the structure, a higher electric field establishs in the current path. Then Avalanche carrier multiplication may occur at the interface states, leading to the usually observed superlinear reverse characteristics of silicon solar cells at higher voltages.

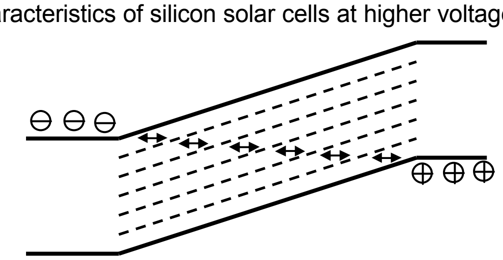

Fig. 7: Schematic drawing of the ohmic conductivity across a continuum of states in an extended defect position.

DISCUSSION

In this contribution we have collected new arguments for explaining the non-ideal shape of the dark I-V characteristics, especially of ideality factor larger than 2 of the recombination current, of most industrial silicon solar cells. There is clear experimental evidence that, even in multicrystalline cells, the overwhelming part of the area of the cells shows an ideality factor close to 1 and a negligible recombination current, in accordance with classical diode theory. The measured recombination current of the cell flows essentially locally in the position of the cell edge and in the position of recombination-induced shunts. In these positions, the local density of states crossing the band gap may be so high that collective recombination mechanisms become probable, and that electrostatic effects cannot be neglected anymore. We have described three of such mechanisms, but there may be also more. The two multi level recombination mechanisms may explain a saturation of the space charge recombination current with increasing forward bias, which may lead to ideality factors larger than 2. We also propose that the linear or superlinear reverse characteristic is due to the same extended defects crossing the pn-junction. In addition, we point to the fact that extended defects with a high density of interface states crossing the pn-junction inevitably lead to electrostatic charging, which alters the field distribution in defect position considerably. A realistic Dessis simulation of a non-passivated edge region has lead to a considerable local extension of the recombination region across the surface. This extension is responsible for edge saturation current densities larger than 10^{-8} A/cm, which cannot be explained without such electrostatic effects.

According to our previous simulations, multi level recombination effects are the basic reason for large ideality factors. However, until now we cannot predict whether the coupled defect-level model or the deep DAP recombination model is more appropriate to describe real edge currents. For more precise predictions we would need more data about the electronic properties of non-passivated surface states. One important indication of the recombination mechanism may be the temperature depencence of the edge recombination current. It had been found, e.g., that the nT product is nearly constant for different edge isolation approaches [16]. By this contribution we also want to encourage the collection of realistic surface or interface state density data. We hope that, with a better theoretical understanding of the dark I-V characteristic of solar cells, also new ways can be found to avoid the still existing problems of solar technology, e.g. concerning shunting and pre-breakdown phenomena.

One of the authors (O.B.) is grateful to the Centre for Photovoltaic Engineering of the University of New South Wales, Sydney, for its hospitality during a working stay in 2003, where these investigations have started. These investigations have been supported by the German BMU project ASIS (project No. 0329846D). One of the authors (A.S.) wishes to thank Dr. Andreas Wettstein (Synopsys Switzerland LLC) for upgrades of the coupled defect level recombination model in Dessis.

References

[1] K.R. McIntosh, P.P. Altermatt, G. Heiser, "Depletion-region recombination in silicon solar cells: when does m_{DR} = 2 ?", Proc.16th EC Solar Energy Conference, Glasgow, UK, pp. 251-254, 2000.

[2] P.P. Altermatt, A.G. Aberle, J. Zhao, A. Wang, G. Heiser, "A numerical model of p-n junctions bordering on surfaces", Solar Energy Materials and Solar Cells 74, pp. 165-174, 2002.

[3] A. Kaminski, J.J. Marchand, H. El Omari, A. Laugier, Q.N. Le, D. Sarti, "Conduction processes in silicon solar cells", Proc. 25th IEEE PVSC, Washington DC 1996, pp. 573-576.

[4] J. Beier, B. Voss, "Humps in dark I-V curves - analysis and explanation", Proc. 23rd IEEE PVSC, Louisville 1993, pp. 321-324.

[5] A. Schenk, U. Krumbein, "Coupled defect-level recombination: Theory and application to anomalous diode characteristics", J. Appl. Phys. 78 (1995), pp. 3185-3192.

[6] H.J. Queisser, "Forward characteristics and efficiencies of silicon solar cells", Solid-State-Electronics 5 (1962) 1-10.

[7] O. Breitenstein, W. Eberhardt, K. Iwig, "Imaging the forward current density of solar cells by dynamical precision contact thermography", Proc. 1st WCPEC, Hawaii 1994, pp. 1633-1636.

[8] O. Breitenstein, M. Langenkamp, "Quantitative local analysis of I-V characteristics of solar cells by thermal methods", Proc. 2nd WCPEC, Vienna 1998, pp. 1382-1385.

[9] O. Breitenstein, M. Langenkamp, J.P. Rakotoniaina, J. Zettner, "The imaging of shunts in solar cells by infrared lock-in thermography", Proc. 17th Eur. PVSEC, Munich 2001, pp. 1499-1502.

[10] O. Breitenstein, J.P. Rakotoniaina, S. Neve, M.A. Green, Jianhua Zhao, Aihua Wang, G. Hahn, "Lock-in thermography investigation of shunts in screen-printed and PERL solar cells", 29th IEEE PVSC, New Orleans 2002, pp. 430-433.

[11] O. Breitenstein, M. Langenkamp, "Lock-in Thermography - Basics and Use for Functional Diagnostics of Electronic Components", Springer (Berlin / Heidelberg / New York) 2003.

[12] O. Breitenstein, J. Heydenreich, "Non-ideal I-V-characteristics of block-cast silicon solar cells", Solid State Phenomena **37-38** (1994), pp. 139-144.

[13] K.R. McIntosh, C.B. Honsberg, "The influence of edge recombination on a solar cell's I-V curve", Proc. 16th PVSEC, Glasgow 2000, pp. 1651-1654.

[14] R. Kühn, P. Fath, E. Bucher, "Effects of pn-junction bordering on surfaces investigated by means of 2D-modeling", Proc. 28th IEEE PVSC, Anchorage 2000, pp. 116-119.

[15] Dessis 10.0 User's Manual, Synopsys Inc., 2005.

[16] M.A. Green, A.W. Blakers, C.R. Osterwald, "Characterization of high-efficiency silicon solar cells", J. Appl. Phys. **58** (1985), pp. 4402-4408.